Analyst

Accepted Manuscript

This is an *Accepted Manuscript*, which has been through the Royal Society of Chemistry peer review process and has been accepted for publication.

Accepted Manuscripts are published online shortly after acceptance, before technical editing, formatting and proof reading. Using this free service, authors can make their results available to the community, in citable form, before we publish the edited article. We will replace this *Accepted Manuscript* with the edited and formatted *Advance Article* as soon as it is available.

You can find more information about *Accepted Manuscripts* in the Information for Authors.

Please note that technical editing may introduce minor changes to the text and/or graphics, which may alter content. The journal's standard Terms & Conditions and the Ethical guidelines still apply. In no event shall the Royal Society of Chemistry be held responsible for any errors or omissions in this *Accepted Manuscript* or any consequences arising from the use of any information it contains.

ROYAL SOCIETY OF CHEMISTRY

www.rsc.org/analyst

Native fluorescence Spectroscopic Characterization of DMBA Induced Carcinogenesis in Mice Skin for the early detection of tissue transformation

Jeyasingh Ebenezar [1, 2], Prakasarao Aruna [1] and Singaravelu Ganesan [1*]

[1]Department of Medical Physics, Anna University, Chennai - 600025, INDIA.
[2]Present Address: Department of Physics, Jamal Mohamed College (Autonomous), Tiruchirappalli – 620020, INDIA.

[*]Corresponding author:

Dr. Singaravelu Ganesan,
Professor
Department of Medical Physics
Anna University
Chennai- 620025
INDIA .

E-mail : sganesan@annauniv.edu

Phone: 91-44-22203154
Fax : 91- 44-22352270

Abbreviations:

NF, Native fluorescence;
DMBA, Dimethylbenz[a]anthracene
ESCC, Early squamous cell carcinoma;
WDSCC, Well differentiated squamous cell carcinoma;
NADH, Nicotinamide adenine dinucleotide;
FAD, Flavin adenine dinucleotide;
PpIX, Protoporphyrin IX;

Analyst Accepted Manuscript

ABSTRACT

The objective of the study is to characterize the endogenous porphyrin fluorescence in dimethylbenz(a)anthracene (DMBA) induced mouse skin tumor model using native fluorescence emission and excitation spectroscopy. Two intensity ratio parameters I_{580}/I_{635} and I_{420}/I_{515} were selected to represent the key fluorophore of endogenous porphyrins from emission and excitation spectra recorded *in vivo* from 31 DMBA treated animals and 5 control animals. In the emission spectrum, the endogenous porphyrin was elevated at 635 nm during different transformation lesions such as hyperplasia, papilloma, dysplasia, ESCC and WDSCC. This is corroborated by the endogenous porphyrin elevation at 420, 515, 550 and 588 nm in the WDSCC lesions from the excitation spectra. The elevation of endogenous porphyrin, probably protoporphyrin IX (PpIX), is due to biochemical and metabolic alterations in epithelial cells during tissue transformation. The loss of ferrochelatase activity might be responsible for enhanced PpIX in the transformed tissues. The sensitivity and specificity were determined for different lesion pairs from the scatter plot based on the discrimination value by validation with histopathological results. The emission intensity ratio I_{580}/I_{635} at 405 nm excitation was selected to discriminate normal from hyperplasia, hyperplasia from papilloma, papilloma from dysplasia, dysplasia from early squamous cell carcinoma (ESCC), and ESCC from well differentiated squamous cell carcinoma (WDSCC) with specificities of 100%, 88%, 100%, 86%, and 100% and sensitivities of 100%, 80%, 100%, 100% and 100% respectively. Similarly, the excitation intensity ratio I_{420}/I_{515} for 635 nm emission to discriminate between WDSCC lesions from normal gives 100% specificity and 100% sensitivity.

Analyst Accepted Manuscript

INTRODUCTION

Over half of all human cancers originate in the stratified squamous epithelia. Examples of tissues with stratified squamous epithelia include the cervix, skin, and oral cavity. Approximately 1 million cases of non-melanoma cancers of the stratified squamous epithelia are identified each year.[1] Hence, early detection and treatment of squamous epithelial cancers is important to minimize morbidity and mortality. Native fluorescence (NF) spectroscopy for cancer detection is a promising technique proposed as "Optical Biopsy" by Alfano in 1984.[2] Later, NF spectroscopy has been considered as one of the powerful techniques because of its sensitivity to metabolic, structural and microenvironmental changes of the various endogenous fluorophores present in the tissues.[3,4] Of the various fluorophores, the fluorescence of collagen, more generally protein, is related to the structural arrangement of cells and tissues. The other fluorophores, NADH, FAD, and endogenous porphyrin are related to metabolic processes.[5] A change in the state of the tissue that occurs during physiological processes or in connection with the onset of pathological conditions, results in modifications of the amount of fluorophores, their distribution, and the biochemical properties of their environment.[4] Among the various optical spectroscopic techniques, native fluorescence spectroscopy has been considered as one of the powerful techniques because of its sensitivity to structural and microenvironmental changes of the various endogenous fluorophores present in the tissues.[5]

A number of clinical investigations carried out on a variety of tissue sites including the cervix,[6] skin,[7] and oral cavity[8] demonstrate that NF provides sensitive and specific

Analyst Accepted Manuscript

detection of squamous epithelial cancer. However, most of the clinical cases are reported for diagnosis after the early neoplastic changes, which are considered as a major drawback in exploring the potentiality of NF technique for the early detection of cancer. Further, it is practically difficult to measure the spectra of a lesion in a patient, during its progression from normal to premalignant and malignant condition. Hence, understanding the fluorescence characteristics from a single site during onset of the neoplastic changes during the tissue transformation sequence is important from the clinical perspective. In this context, mouse skin carcinogenesis model has the potential to provide a better understanding of how fluorescence spectra are changing during normal tissue progresses through dysplasia to cancer sequence. Several *in vitro* and *in vivo* studies have been performed in which squamous cell carcinoma initiated with 7,12 dimethyl benz(a)anthracene (DMBA) induced hamster cheek pouch/skin carcinogenesis and then NF characterization of the tissue transformation was measured.[9-12] However, to the best of our knowledge, no comparison of histological categorization of various tissue transformation conditions with respect to normal tissues in mice skin carcinogenesis model for measuring emission spectrum at 405 nm excitation and excitation spectrum at 635 nm emission has been made till date. Therefore, the novelty of this study is that for the first time a NF spectroscopy using a selective combination of specific emission and excitation wavelengths, mentioned above has been made for measuring various tissue transformation conditions in mice skin carcinogenesis *in vivo*.

Analyst Accepted Manuscript

The aim of the present study is to (i) characterize the NF emission and excitation spectral measurements of mice skin during the tissue transformation process (0-18 weeks). (ii) classify the spectral profiles of the each biopsy site for different histological category. (iii) identify the spectral intensity ratio variables based on the observed fluorescence emission peaks at 405 nm excitation and fluorescence excitation peaks at 635 nm emission. (iv) use these ratio variables to classify normal from various tissue transformation process statistically.

MATERIALS AND METHODS

Animals

For the present study, 36 Swiss Albino mice, both male and female, 6-8 weeks old at the start of the experiment were obtained from National Institute of Nutrition, Hyderabad, India. At the beginning of the study, all animals weighed approximately 25-30 g each. The animals were housed four per cage with a right diet but ad libitum access to food and water. The animals were maintained at 27°C with 12 hours dark/light cycle. Animals care and procedures were in accordance with guidelines of ethical committee, Government of India.

Mice Skin Carcinogenesis Model

At the beginning of the experiment, all hair of the animals on their dorsal side approximately 1 cm^2 were removed with a hair removing cream (Anne French, Geoffrey manners and Co. Ltd., Mumbai, India). On confirmation of no scar on the skin surface, they were subjected to tumor induction. Healthy animals were divided into two groups. One group of animals treated for epithelial carcinogenesis (n=31) and other consisted of control animals (n=5). The first group was treated with 0.5% of DMBA in heavy mineral oil (Sigma Aldrich Co., St. Louis, Missouri) thrice a week during the first 3 weeks. However, from the fourth week,

Analyst Accepted Manuscript

treatment was reduced to twice per week due to the reddening and erosion of the skin. The control group was treated only with heavy mineral oil. Separate No.5 camelhair brushes were used for the topical application of DMBA/mineral oil solution on the epithelial carcinogenesis group and mineral oil alone on the control group. The carcinogen treatment was carried out for a period of 18 weeks.

Instrumental Description

In vivo fluorescence of emission and excitation spectral measurements was recorded using a spectrofluorometer with a Y-guide fiber optic probe (Fluoromax-2, ISA, Jobin Yvon-Spex, Edison, New Jersey, USA) of their schematic instrumentation is shown Fig.1. The excitation source (150 W Ozone free Xenon arc lamp) coupled to the monochromator delivers light to a fiber optic probe coupled to one end of the Y-wave guide fiber. The other end of the fiber collecting the signal was coupled to the emission monochromator connected to a photomultiplier tube (PMT; R928P, Hamamatzu, Shizuoka-Ken, Japan). The collected signal is transferred to the PC through an RS232 interface, and processed by the windows-based data acquisition program, DataMax (ISA, Jobin Yvon-Spex). The excitation and collection end of the fiber assembly were connected to the excitation and emission monochromators, respectively. The fiber optic assembly (~8 mm outer diameter) contained 31 delivery and 31 collection fibers of 250 μm diameter randomly mixed. A flexible spacer 1 cm long, disposable, black PVC sleeve was inserted at the common end of the fiber-optic probe assembly maintains a fixed separation of approximately 0.5 cm between the probe tip and tissue surface. The common end of the fiber tip was mounted perpendicularly on XYZ micrometer translational stage for precise location and for prevention of handheld tremor during measurements.

Analyst Accepted Manuscript

The emission spectral measurements of control and DMBA treated mice skin were recorded between 430–700 nm for the excitation wavelength of 405 nm for which the excitation and the emission wavelength band passes were 2 and 3 nm respectively with integration time of 0.1 sec. For the excitation spectra recorded between 340–600 nm at an emission wavelength of 635 nm, the excitation and emission band passes were set at 5 and 3 nm respectively with the integration time being the same as that of emission spectral measurements. The excitation wavelength for 405 and 635 nm from the spectrometer was low in intensity, which is about 2–5 $\mu w/cm^2$, and did not induce any significant photobleaching of endogenous porphyrin. Prior to start of each measurement day, a background spectrum was obtained at each excitation and emission wavelength by inserting the probe into a nonfluorescent bottle filled with distilled water. The background spectrum was then subtracted from the corresponding tissue fluorescence spectrum.

Mice Skin Fluorescence Measurements

Two groups of live animals were monitored on a weekly basis periodically for 18 weeks for any changes in their NF emission and excitation characteristics using a fiber-optic probe based spectrofluorometer. In order to avoid residual fluorescence due to DMBA application, the experiments were designed in such a way that, the florescence measurements always took place at least 48 hrs after DMBA treatment.[10] Before optical measurements, the tumor induction site of the mice skin was swabbed with saline and cleaned dry with a piece of sterilized cotton. Using translational XYZ micrometer, the probe with spacer was moved into at least three different sites of the tumor induction area of each animal and subsequently optical measurements were recorded. Among the three sites of each animal in the DMBA

Analyst Accepted Manuscript

treated group, that site showing more porphyrin fluorescence was marked for biopsy and subsequently that animal was sacrificed that week. The biopsy site of the corresponding emission and excitation spectral measurements of that animal was taken out for data analysis. Likewise, at least one or two animals were selected from the DMBA treated group and were sacrificed every week and the skin was removed surgically for histopathological evaluation. Similarly, each one of the control group animals was periodically sacrificed. The periods of sacrifice of the DMBA treated mice and control group were noted.

Histological Evaluation

At different time periods (1 to 18 weeks) during the tumor induction, animals were euthanized by over dosage of isofluorane (5%). Following euthanasia, the tissue specimens were excised from the tumor induction spot of the measured site, using 2 mm biopsy punch and preserved in 10% formalin solution for hematoxylin and eosin (H&E) and submitted for histological evaluation.

Data Analysis

The skin samples of 36 mice were classified into six different groups based on the histopathology report which indicated that a biopsy site of the mice was normal, and then the measurements on that date of mice data were assumed to be normal. The skins of the five control mice were treated only with mineral oil, all were diagnosed as histologically normal. Similarly, the spectroscopic data of the DMBA treated animals were classified into five groups according to their histopathology report. For example, if histopathology indicated that a biopsied site was hyperplasia then the measurements on that date of mice data were assumed to be hyperplasia. Similarly, we obtained the data for papilloma, dysplasia, ESCC and WDSCC in the different weeks of DMBA treated periods. The number

Analyst Accepted Manuscript

of animals as well as the number of spectra obtained from the control and different tissue transformation of the DMBA treated group for the data analysis and different periods of sacrifice week are shown in Table 1. Of the 31 DMBA treated mice skins were assumed to be diagnosed as 8 had hyperplasia, 5 had papilloma, 7 had dysplasia, 6 had ESCC, and 5 had WDSCC.

The purpose of measuring the three sites of each animal is to identify the accurately transformed site by measuring the porphyrin fluorescence. The site showing the highest porphyrin fluorescence was marked for biopsy and sent for histopathalogical evaluation. For cross-verification, the other two sites which did not show porphyrin fluorescence were also biopsied and sent for histopathological evaluation, but no definite histological changes were observed. Hence, other two sites were not included in the spectral and classification analysis. In the present study each animal was subjected to histological evaluation during the tissue transformation process and the spectral profiles of each histological category were grouped for the classification analysis. A few of the spectral data were discarded due to artifacts because of animal movement, probe pressure and angulations during the measurement, resulting in reducing the total to 36 mice of skin samples.

Each fluorescence emission and excitation spectrum was normalized individually to the maximum fluorescence intensity of the each spectrum. Each normalized spectral group of normal and different tissue transformation groups of hyperplasia, papilloma, dysplasia, ESCC, and WDSCC were averaged separately. However, in order to identify the exact spectral differences between normal and various tissue transformation groups, the difference spectrum was also computed by subtracting each normalized average fluorescence emission spectra of hyperplasia (H), papilloma (P), dysplasia (D), ESCC (E) and WDSCC (W) from

Analyst Accepted Manuscript

normal (N) tissues. Like that, the difference spectrum was generated as (N-H), (N-P), (N-D), (N-E), and (N-W) for emission spectrum at 405 nm excitation and excitation spectrum at 635 nm emission were shown in Figures 2 (a-e) and 3 (a-e) respectively.

Statistical Analysis

In order to verify the diagnostic potential of these observed spectral signatures between normal and various tissue transformation conditions, five ratio parameters I_{480}/I_{550}, I_{480}/I_{580}, I_{480}/I_{635}, I_{550}/I_{580}, and I_{580}/I_{635} for emission spectra at 405 nm excitation and three ratio parameters I_{420}/I_{515}, I_{515}/I_{550}, and I_{550}/I_{585} for excitation spectra at 635 nm emission were generated. The mean and standard deviation values of all the experimental group of subjects were calculated and their statistical significance was verified using one-way Analysis of Variance (ANOVA) with 95% confidence interval.

The classification analysis for the different tissue transformation groups were determined on the basis of discrimination cut-off (threshold) values. Discrimination cut-off lines are drawn between the normal (mean of all normal tissues) and hyperplastic (mean of all hyperplastic tissues), hyperplastic and papilloma, papilloma and dysplasia, dysplasia and ESCC, ESCC and WDSCC, at values that correspond to the mean ratio value of the respective groups. The sensitivity and specificity in discriminating each of these categories were determined on the basis of the cut-off values identified by ratio method by validation with histopathological results of biopsy specimens taken from spectral measurements sites. Similar ratio intensity variable methods and the sensitivity and specificity were determined on the basis of the discrimination cut-off lines adopted by earlier researchers to discriminate normal from different tissue categories of oral and bladder tissues. [8,13]

Analyst Accepted Manuscript

RESULTS

Fluorescence Emission Spectral Characteristics at 405 nm Excitation

The normalized average fluorescence emission spectrum of normal and DMBA treated skin lesions such as hyperplasia, papilloma, dysplasia, ESCC and WDSCC with their corresponding difference spectrum at 405 nm excitation is shown in Figures 2(a-e). The normalized average fluorescence emission spectrum of normal tissue has a primary peak around 470 nm with a small shoulder observed at 550 nm and then it decreases towards longer wavelengths with a small hump at 635 nm. In the case of DMBA treated skin, the amplitude of the hump at 635 nm increases with respect to normal tissues. Further, the intensity of peak emission wavelength at 635 nm increases as the stage of skin transformation increases. The difference spectrum between normal and hyperplasia (N-H), and normal and papilloma (N-P), and normal and dysplasia (N-D) skin condition has primary negative peak around 480 nm and a secondary peak at 635 nm (Figures 2a, 2b & 2c), whereas in the case of difference spectrum between normal and ESCC (N-E), and normal and WDSCC (N-W) skin condition, it has a maximum negative peak at 635 nm and minimum broad peak around 480 nm with an isosbestic point at 580 nm (Figures 2d & 2e).

Fluorescence Excitation Spectral Characteristics for 635 nm Emission

The normalized average fluorescence excitation spectrum of normal and various skin transformation condition such as hyperplasia, papilloma, dysplasia, ESCC and WDSCC with their corresponding difference spectrum at 635 nm emission is shown in Figures 3(a-e). From these excitation spectra, it was found that there was a little amount of increased fluorescence intensity throughout the wavelength region (350–600 nm) with small hump was observed around 450 nm for hyperplasia, papilloma, dysplasia, ESCC than normal

Analyst Accepted Manuscript

tissues. The corresponding difference spectrum also shows, there was no appreciable differences were found out between (N-H), (N-P), (N-D), and (N-E) groups (Figures 3a, 3b, 3c & 3d). However, the excitation spectra of WDSCC lesions displayed a prominent primary band at 420 nm and three secondary spectral bands at 515, 550 and 588 nm respectively (Figure 3e). But these bands were completely absent in the case of normal, hyperplasia, papilloma, and ESCC skin lesions. The corresponding difference spectrum shows an apparent difference between normal and WDSCC (N-W) skin lesions has a maximum negative peak at 420 nm and three minimum peaks at 515, 548 and 585 nm.

Results of Histological Evaluation

In order to confirm the different morphological changes that occur during the sequential tissue transformation process, animals were sacrificed at different time periods for histological evaluation. Histological images of the mouse skin at different periods are shown in Figures 4(a-f). Five control mice skin (treated only with mineral oil) were all diagnosed as histologically normal. The histological normal mouse skin shows thin epithelial layer with intact collagen matrix. Further, epidermis and the dermis contain numerous hair follicles (Fig. 4a). Of the 31 DMBA treated mice skin 8 had hyperplasia, 5 had papilloma, 7 had dysplasia, 6 had ESCC and 5 had WDSCC. According to the histopathology report, from the DMBA treated skin was separated by five transformation conditions. (1) During 4-6 weeks of DMBA treatment, the skin appeared thick and reddened whiles the histology of the skin showed hyperplastic changes (i.e) increased thickness of epithelium with the indications of moderate hyperplastic and the early stage of papillary hyperplasia (Fig. 4b). (2) During 5-9 weeks, papillomatous outgrowths were noticed that was confirmed by the histopathology showing papillomatous proliferation of the epidermis (Fig. 4c). (3) At about 10-13 weeks,

Analyst Accepted Manuscript

the skin lost its normal orientation between the epithelial cells leading to dysplastic stratified squamous epithelium (Fig. 4d). (4) Numerous nodular growths were seen during 14-16 weeks. Atypical squamous cells replaced the entire epithelium giving histology of early invasive squamous cell carcinoma (Fig. 4e). (5) After 17-18 weeks, the tumor grew larger in size with features of well-differentiated squamous cell carcinoma, demonstrating invasion of tumor cells into the dermis with atypical mitoses and keratin pearls were also seen (Fig. 4f).

Results of Statistical Analysis

Among five ratio parameters (I_{480}/I_{550}, I_{480}/I_{580}, I_{480}/I_{635}, I_{550}/I_{580}, and I_{580}/I_{635}), the ratio parameter I_{580}/I_{635} was identified as the most significant (P<0.0001) ratio in discriminating the normal from different tissue transformation conditions for emission spectrum at 405 nm excitation. The intensity I_{580} has been chosen to represent the hemoglobin absorption and I_{635} represent the characteristic emission because of endogenous porphyrin. The mean and standard deviations of the ratio parameter (I_{580}/I_{635}) for normal and different tissue transformations are shown in Table 2. It can be seen that the mean value of the normal group is high but there is a gradual decrease in the mean values according to the progression to higher grades of malignancy. Similarly, out of three ratio parameters (I_{420}/I_{515}, I_{515}/I_{550}, and I_{550}/I_{585}), the ratio parameter I_{420}/I_{515} was identified as the most significant (P<0.0001) ratio in discriminating the normal from WDSCC lesions for excitation spectra at 635 nm emission. This intensity ratio value corresponds to soret band (I_{420}) and Q-band (I_{515}). Mean standard deviation of the ratio parameter (I_{420}/I_{515}) for normal and WDSCC lesions also shown in Table 2, from which the mean value of normal is low and it increases for WDSCC lesions.

Analyst Accepted Manuscript

The ratio parameter (I_{580}/I_{635}) showed best discrimination not only between normal and malignant but also between different tissue transformation conditions such as (a) normal vs hyperplasia (b) hyperplasia vs papilloma (c) papilloma vs dysplaisa (d) dysplasia vs ESCC (e) ESCC vs WDSCC for emission spectrum at 405 nm excitation. Discrimination lines were drawn between contiguous normal-hyperplasia, hyperplasia–papilloma, papilloma–dysplasia, dysplasia–ESCC, and ESCC–WDSCC groups at values that correspond to the mean ratio values of the respective groups. The discrimination (cut-off) value in the scatter plot which is the weighted mean of the paired values was used to classify different lesions. There are five cut-off lines in Fig. 5. The cut-off values for normal–hyperplasia, hyperplasia–papilloma, papilloma–dysplasia, dysplasia-ESCC, and ESCC-WDSCC pairs are 1.07, 0.97, 0.81, 063, and 0.55 respectively. Diagnostic accuracies such as specificity and sensitivity for each pair were calculated by correlating the position of ratio value for each lesion in the scatter plot (Fig. 5) with the corresponding histopathological results given in Table 3. For example, the I_{580}/I_{635} ratio, the first cut-off line discriminating the normal from the hyperplasia was drawn at 1.07 that corresponds to mean of normal (1.14) and that mean of hyperplastic (0.99) group gives 100% specificity and 100% sensitivity was obtained for discrimination of the normal from hyperplasia. The second cut-off line drawn at 0.97 that corresponds to mean of hyperplasia (0.99) and that mean of papilloma (0.94) discriminates the hyperplasia from papilloma with the specificity and sensitivity of 87.5% and 80% respectively. In this classification analysis, only 1 of 8 hyperplastic tissues was misclassified as papilloma, and 1 of 5 papilloma tissues was misdiagnosed as hyperplasia. The third cut-off line drawn at 0.81 that corresponds to mean of papilloma (0.94) and that mean of dysplasia

Analyst Accepted Manuscript

(0.68) group gives 100% specificity and 100% sensitivity was obtained for discrimination of the papilloma from dysplasia. In the same plot, fourth cut-off drawn at 0.63 that corresponds to mean of dysplasia (0.68) and that mean of ESCC (0.58) group discriminates the dysplasia from ESCC with the specificity and sensitivity of 85.7% and 100% respectively. In this analysis, only 1 of 7 dysplastic tissues was misclassified as ESCC. Finally, fifth cut-off line drawn at 0.55 that corresponds to mean of ESCC (0.58) and that mean of WDSCC (0.51) group gives 100% specificity and 100% sensitivity was obtained for discrimination of the ESCC from WDSCC.

Similarly, a single classification analysis was performed between the group of normal vs WDSCC skin lesions for fluorescence excitation spectrum at 635 nm emission. Fig. 6 represent the scatter plot of the intensity ratio of I_{420}/I_{515}, the cut-off line drawn at 3.82 that corresponds to mean of normal (2.23) and WDSCC (5.41) group gives 100% specificity and 100% sensitivity was obtained for the discrimination of normal from WDSCC (Table 3).

However, the 4 ratio parameters such as I_{480}/I_{550}, I_{480}/I_{580}, I_{480}/I_{635}, and I_{550}/I_{580} from emission spectra at 405 nm excitation and two ratio parameters such as I_{515}/I_{550}, and I_{550}/I_{585} from excitation spectra at 635 nm emission have not been included in the Tables 2 and 3, since these parameters did not show good discrimination (less specificity and less sensitivity) at less significance level compared with the ratio parameters I_{580}/I_{635}, and I_{420}/I_{515}.

Analyst Accepted Manuscript

DISCUSSION

Early detection of premalignant and malignant lesions may reduce patient morbidity and mortality because treatment at a less invasive stage is more successful, and therefore is of great clinical importance. In the present study, the NF characterization of sequential tissue transformation in a DMBA induced mouse skin carcinogenesis model was explored and the spectral data were analyzed using a statistical method for better discrimination of normal from the early stages of neoplastic conditions.

Fig. 2(a-e) shows the primary NF emission band at 470 nm and a small hump at 550 nm may be attributed to emission from fluorophores like NADH and FAD respectively, while the emission at 635 nm is from enhanced occurrence of endogenous porphyrin present in different tissue transformation lesions. An increased NADH fluorescence in hyperplasia, papilloma, dysplasia, ESCC and WDSCC due to proliferation of cells could be the result of an increased metabolic activity associated with progression of neoplastic changes. The corresponding difference spectra of the different tissue transformation lesions showed a parabolic curve of spectral profile with the negative peak observed at 480 nm. On the whole, the difference spectrum between N-H, N-P, N-D, N-E, and N-W reveals increased NADH fluorescence when compared with normal lesions. Further, it is evident that the NADH emission which increases at 470 nm during the tissue transformation could be well appreciated in the overall emission spectrum (Fig.7). These observations indicate increased level of NADH during the neoplasitc progression due to (i) rapidly multiplying neoplastic cells with increased metabolic activity,[12] (ii) decreased blood flow due to the rapid cell division,[14-16] (iii) decrease in oxygen supplied to the

Analyst Accepted Manuscript

cells.[14-16] Further, it is noticed that the increased metabolic activity during the neoplastic transformation is highlighted by an enhanced FAD emission at 550 nm, when compared with normal lesions. Hence, the concentrations and distributions of coenzymes NADH and FAD correlate with the metabolic and physiological states of cells and tissues.

In addition to the NADH and FAD emission, the fluorescence emission spectra of different tissue transformation condition exhibit a distinct emission peak at 635 nm, which is absent in the case of normal mice skin [Fig. 2(a-e)]. It is noted that, the intensity of the emission peaks at 635 nm increases as the skin lesions changes from normal into different stages of tissue transformation namely: hyperplasia, papilloma, dysplasia, ESCC and WDSCC. The corresponding difference spectra show a prominent negative peak at 635 nm, and this peak is going down steeper and steeper as the stages of tissue transformation increase. The additional fluorescence peak at 635 nm observed after DMBA application is attributed to endogenous porphyrin.[9,12] Earlier literature reported that porphyrins have been associated mainly with ulcerating tumors, because of the bacteria that grow in these tissues.[18,19] This phenomenon has been reasonably excluded in the present study since the mice skin did not display any ulceration. As there is no sign of an ulceration seen in the mouse skin there is a systematic increase at 635 nm due to endogenous porphyrins that accumulate and concentrate in viable tumor tissues. The accumulation and retention of endogenous porphyrin in the viable tumor tissues is confirmed by the earlier report on the tissue extracts from DMBA induced hamster cheek pouch and mouse skin tumor exhibiting typical porphyrin fluorescence at 635 nm.[9,20] This systematic porphyrin emission which increases at 635 nm during the tissue transformation could be well appreciated in the overall emission spectrum displayed in

Analyst Accepted Manuscript

Fig. 7. In this spectra, it is evident that the amount and rate of endogenous porphyrin accumulation increases with increasing degree of malignancy. This is due to chronic application of DMBA to the mouse skin; the cellular proliferative activity increases during malignant transformation leading to biochemical and metabolic alterations in epithelial cells affected by the changes that occur during tissue transformation.[21] These changes can modify the synthesis of endogenous porphyrin, probably protoporphyrin IX (PpIX), which preferentially accumulates in tumor cells due to changes in the activity of two main enzymes: porphobilinogen deaminase (PBG) and ferrochelatase (FC).[22] In tumor cells, while the activity of PBG increases, the activity of FC decreases resulting in the building up of PpIX. But in normal cells, FC catalyses the conversion of photosensitive PpIX to heme, which is not photosensitive.[22-24]

A small bump noticed in the emission spectra at 666 nm from normal and DMBA treated mice skin may be due to the degradation products of *chlorophyll a*, namely, *pheophytin a* and *pheophorbide a* present in the food pellets.[25,26]

In order to confirm the origin of the red emission peak at 635 nm observed in the fluorescence emission spectra of DMBA treated animals at 405 nm excitations, the fluorescence excitation spectra were also measured at 635 nm emission for both normal and DMBA treated animals. These are shown in Fig. 3(a-e). The normal and different tissue transformation lesions shows sharp spectral peaks at 362 and 387 nm due to Rayleigh scattering effect and stray light contribution from the excitation light. In the case of hyperplasia, papilloma, dysplasia and ESCC lesions exhibits a small hump was observed around 430–460 nm may be attributed to absorption band of FAD. However,

Analyst Accepted Manuscript

the WDSCC lesion revealed a prominent primary band at 420 nm and three secondary spectral bands around 515, 550 and 588 nm respectively. The band around 420 nm is predominant when compared with the other bands. These observed primary and secondary bands correspond to soret and Q-band absorption of endogenous porphyrins respectively.[5,19] Further, this observed spectral signature of the WDSCC lesions resembles the typical absorption spectra of the porphyrin molecule, it indicates that higher amount of porphyrins synthesized in WDSCC lesions than other transformation conditions. This finding is consistent with the previous work by Ebenezar *et al*, who found out that similar soret and Q-bands were observed in WDSCC of buccal mucosa of oral cancerous patients at 635 nm emission by fluorescence excitation spectroscopy *in vivo*.[27]

Although the NF signal shows distinct differences in the spectral signatures, an *in vivo* quantitative estimation of the different fluorophores at different tissue pathological conditions to discriminate different stages of tissue transformation process is complex due to the tissue heterogeneity and the dependency of fluorescence signal on the tissue optical properties. For instance, optical behaviour of tissue will be highly affected by thickening of skin or change in tissue vascularization that occurs during tissue transformation.[12,21,28,] This highly correlates with the present study of the difference spectrum of hyperplasia from normal, papilloma from normal, and dysplasia from normal (Fig. 2a, 2b & 2c) shows a primary negative peak around 480 nm which corresponds to NADH and a secondary peak at 635 nm due to porphyrin. On the other hand, the difference spectra of the ESCC from normal and WDSCC from normal (Fig. 2d & 2e), show a primary negative peak at 635 nm and a secondary peak around 480 nm with an isosbestic point at 580 nm. From these difference

Analyst Accepted Manuscript

spectra it is strongly inferred that the NADH level increased during initial transformations such as hyperplasia, papilloma and dysplasia lesions. However, with an increase in the degree of malignancy as in the case of both ESCC and WDSCC lesions, the NADH level decreased in intensity compared with hyperplasia, papilloma and dysplasia lesions. The variations in the relative distribution of NADH and porphyrins in the emission spectra corresponding to 405 nm excitation during the tissue transformation process may be due to (i) in the early weeks of DMBA initiation, the inflammatory response is triggered in the skin, thereby increasing the metabolic activity of the inflammated cells, leading to increased level of NADH in the early tissue transformation conditions namely hyperplasia, papilloma and dysplastic lesions,[28] and (ii) during the degree of differentiation increases due to chronic application of DMBA in the mouse skin; the NADH decreases leading to an increased level of porphyrin in the malignant transformation of ESCC and WDSCC lesions.[29,30]

Another possible reason for the decreased NADH intensity due to increased tissue vasculature observed on ESCC and WDSCC tissues, when the animals had a nodular outgrowth of the tumor volume increase in size and varying around 5-8 mm diameter during 14–18 weeks of DMBA treatment**.** As a result, a prominent spectral valley or dip in the emission spectrum around 580 nm is observed as shown in Fig. 2(a-e). This valley is more pronounced in ESCC and WDSCC than hyperplasia, papilloma and dysplastic tissues. In addition to this, an isosbestic point in the difference spectrum was found to occur at 580 nm due to higher hemoglobin absorption and strong porphyrin emission at 635 nm from ESCC and WDSCC tissues (Fig. 2d & 2e). This correlates with the results reported earlier by Van der Breggen *et al.* found out that an increased vascularization of the neoplastic tissues leads

Analyst Accepted Manuscript

to a higher hemoglobin concentration, and also it may contribute to an increase in the rate and amount of porphyrin emission in DMBA treated animal tissues.[21]

Table 3 summarizes the specificity and sensitivity obtained across different histological categories of experimental groups from the scatter plot (Fig. 5) using emission spectral intensity ratio (I_{580}/I_{635}) at 405 nm excitation. The specificities obtained for (a) normal–hyperplasia, (b) hyperplasia–papilloma, (c) papilloma–dysplasia, (d) dysplasia–ESCC, and (e) ESCC–WDSCC pairs are 100%, 88%, 100%, 86% and 100% respectively and the corresponding sensitivities are 100%, 80%, 100%, 100%, and 100% respectively. The reduced specificity and sensitivity from the classification analysis (b & d) was obtained because of some of the hyperplasia, papilloma and dysplasia subjects were misclassified during the earlier weeks of tumor induction. Even one sample was misclassified in the classification analysis (b & d), the specificity and sensitivity was greatly reduced. If the number of sample size is to be increased in these categories, the classification accuracy can be increased. Also the table 3 shows that the 100% specificity and 100% sensitivity was obtained from the scatter plot (Fig. 6) for single lesion pair (normal-WDSCC) for intensity ratio of I_{420}/I_{515} at 635 nm emission.

Although, the present NF study is used to characterize the endogenous porphyrin fluorescence for normal and different tissue transformation, the reflectance spectral measurements were not investigated. The reflectance spectrum is used to assess the changes in the scattering and absorption properties of tissues. To potentially improve the diagnostic accuracy of different tissue transformation, fluorescence spectroscopy in combination with reflectance measurements would be necessary in future. Such investigations with a larger number of animals for normal and different tissue transformation process could be validated in a blinded manner.

Analyst Accepted Manuscript

CONCLUSION

The spectral signatures of the current study demonstrated that NADH, FAD, hemoglobin and porphyrin changes have good diagnostic potential which were elicited at 405 nm excitation. In particular, the significant contribution of porphyrin can be used as a tumor marker. Further, it is confirmed that the porphyrin elevated in the WDSCC tissues from excitation spectra at 635 nm emission. Finally, the intensity ratio parameters I_{580}/I_{635} and I_{420}/I_{515} represent the key fluorophore of porphyrin to diagnose the early tissue transformation process.

Acknowledgments

This work was supported in part by Department of Science Technology (DST) Project No. SP/S2/L-14/96, and All India Council for Technical Education (AICTE) Project No. 8017/RDII/R&D/TAP(881)/98-99, Government of India. The author Jeyasingh Ebenezar thanks the Department of Science and Technology, Govt. of India, New Delhi for the award of Junior Research Fellowship and Dr. Subbulakshmi Annamalai, Department of Pathology, Madras Medical College, Chennai, for her help in histopathologic evaluation.

Analyst Accepted Manuscript

REFERENCES

1. Cancer facts and figures. Atlanta (GA): American Cancer Society (2003).
2. R.R. Alfano, D.B. Tata, J. Cordero, P. Tomashefsky, F.W. Longo, and M.A. Alfano, *IEEE J.Quantum Electron*., 1984, 23, 1507–1511.
3. S. Andersson-Engels, J. Johansson, K. Svanberg, and S. Svanberg, *Photochem. Photobiol.,* 1990, 53, 807–814.
4. R. Richards-Kortum, and E. Sevick-Muraca, *Annu. Rev. Phys. Chem.,* 1996, 47, 555–606.
5. N. Ramanujam, In: Meyers RA (ed.), *Encyclopedia of analytical chemistry*, John Wiley & Sons, Chichester, 2000, pp. 20–56.
6. A. Mahadevan, M. F. Mitchell, E. Silva, S. Thomsen, and R. Richards-Kortum, *Laser Surg. Med.,* 1993, 13, 646–655.
7. L. Brancaleon, A.J. Durkin, J.H. Tu, G. Menaker, J.D. Fallon, and N. Kollias, *Photochem. Photobiol.,* 2001, 73(2), 178–183.
8. R.J. Mallia, S.S. Thomas, A. Mathews, R. Kumar, P. Sebastian, J. Madhavan, and N. Subhash, *Cancer,* 2008, 112, 1503–1512.
9. N. Vengadesan, P. Aruna, and S. Ganesan, *Br. J. Cancer,* 1998, 77(3), 391–395.
10. L. Cohlan, U. Utinger, R. Richards-Kortum, C. Brookner, A. Zuluga, I. Gimenez-Conti, and M. Follen, *Lasers Surg. Med.,* 2001, 29, 1–10.
11. M.C. Skala, G.M. Palmer, C. Zue, Q. Liu, K.M. Vrotsos, C.L. Marshek-stone, A. Gendron-Fitzpatrick, and N. Ramanujam, *Lasers Surg. Med.,* 2004, 34, 25–38.
12. P. Diagaradjane, M.A. Yaseen, J. Yu, M.S. Wong, and B. Anvari, *Lasers Surg. Med.,* 2005, 37, 382–395.

Analyst Accepted Manuscript

13. W. Zheng, W. Lau, C. Christopher, K.C. Soo, and M. Oliva, *Int. J. Cancer,* 2003, 104, 477–481.

14. C.J. Gulledge and M.W. Dewhirst, *Anticancer Res*., 1996, 16(2), 741-749,

15. B. Chance, *J. Appl. Cardiol*. 1989, 4(4), 207-221.

16. B.W. Pogue, J.D. Pitts, M.A. Mycek, R.D. Sloboda, C.M. Wilmot, J.F. Brandsema, and J.A. O'Hara, *Photochem. and Photobiol.* 2001, 74(6), 816-824.

17. D.M. Harris, and J. Werkhaven, *Lasers Surg. Med.*, 1987, 7, 467- 472.

18. D.C.G. De Veld, M.J.H. Witjes, H.J.C.M. Sterenborg, and J.L.N. Roodenburg, *Oral Oncol.*, 2005, 41, 117-131.

19. K. Koenig and H. Schneckenburger, *J. of Fluores.,* 1994, 4(1), 17- 40.

20. P. Diagaradjane, S.K. Pushpan, A. Srinivasan, M. Ravikumar, T.K. Chandrashekar, and S. Ganesan, *Photochem. Photobiol.,* 2003, 78, 487–495.

21. E.W.J. Vand er Breggen, A.I Rem, M.M. Christian, C.J. Yang, K.H. Calhoun, H.J.C.M. Sterenborg, and M. Motamedi, *IEEE J. Sel. Top. Quantum Electron.,* 1996, 2, 997–1007.

22. R. Van Hillegersberg, J.W.O. Van den Berg, W.J. Kort, O.T. Terpstra, and J.H.P. Wilson, *Gasteroenterol.,* 1992, 103, 647-651.

23. K.T. Moesta, B. Ebert, T. Handke, D. Nolte, C. Nowak, W.E. Haensch, R.K. Pandey, T.J. Dougherty, H. Rinneberg, and P.M. Schlag, *Cancer Res.* 2001, 61, 991-999.

24. W. Kemmner, K. Wan, S. Ruttinger, B. Ebert, R. Macdonald, U. Klamm, and K.T. Moesta, *FASEB J*, 2008, 22, 500-509.

Analyst Accepted Manuscript

25. G. Weagle, P.E. Paterson, J.C. Kennedy, and R.H. Pottier, *J. Photochem. Photobiol. B: Biol.,* 1998, 2, 313–320.

26. J.T.H.M. Van den Akker, O.C. Speelman, H.J. Van Staveren, A.L. Moore, T.A. Moore, D. Gust, W.M. Star, and H.J.C.M Sterenborg, *J. Photochem. Photobiol. B: Biol.,* 2000, 54, 108–115.

27. J. Ebenezar, S. Ganesan, P. Aruna, R. Muralinaidu, K. Renganathan, and T.R. Saraswathy, *J. Biomed. Opt.,* 2012,17(9), 097007.

28. P. Diagaradjane, M.A. Yaseen, J. Yu, M.S. Wong, and B. Anvari, *J. Biomed. Opt.,* 2006, 11(1), 014012.

29. I. Pavlova, K. Sokolov, R. Drezek, A. Malpica, M. Follen, and R. Richards-Kortum, *Photochem. Photobiol.,* 2003, 77(5), 550–555.

30. J.L. Jayanthi, N. Subhash, M. Stephen, E.K. Philip, and V.T. Beena, *J. Biophoton.,* 2011, 4(10), 696–706.

Analyst Accepted Manuscript

TABLES

Table 1. Histological Assessment Results of 36 Tissue Sites.

Histological diagnosis	Period of sacrifice week	Number of spectra / number of animals	Number of weeks DMBA treated
Normal	0–18	5	N/A
Hyperplasia	4–6	8	4.5±0.8
Papilloma	5–9	5	7.4 ±1.5
Dysplasia	10–13	7	11.5±0.9
ESCC	14–16	6	15±0.8
WDSCC	17–18	5	18 ± 0.7

Analyst Accepted Manuscript

Table 2. Mean values (± SD) of the ratio parameter from emission and excitation spectrum for normal and different tissue transformations used for statistical analysis. Their statistical significance (*p*) between each contiguous group was verified by unpaired student's *t*-test. For I_{580}/I_{635}, the *p*-value of normal vs hyperplasia, papilloma vs dysplasia, dysplasia vs ESCC, and ESCC vs WDSCC is 0.000. But for, hyperplasia vs papilloma is 0.091. For I_{420}/I_{515}, the p-value of normal vs WDSCC is 0.000.

Different tissue transformation	**Mean ± SD**	
	Emission Spectrum	**Excitation Spectrum**
	I_{580}/I_{635}	**I_{420}/I_{515}**
Normal	1.14±0.03	2.23±0.15
Hyperplasia	0.99±0.02	
Papilloma	0.94±0.05	
Dysplasia	0.68±0.04	
ESCC	0.58±0.01	
WDSCC	0.51±0.01	5.41±0.32

Analyst Accepted Manuscript

Table 3. Specificity and Sensitivity Obtained for Different Lesion Pairs Consisting 36 Mice Skin Samples for Intensity Ratio of I_{580}/I_{635} at 405 nm Excitation and Single lesion Pair Consisting 10 Samples for Intensity Ratio of I_{420}/I_{515} at 635 nm Emission.

Lesion Pairs	405 nm Excitation		Lesion Pair	635 nm Emission	
	I_{580}/I_{635}			I_{420}/I_{515}	
	Specificity	Sensitivity		Specificity	Sensitivity
Normal(5) vs Hyperplasia(8)	100%	100%	Normal(5) vs WDSCC(5)	100%	100%
Hyperplasia(8) vs Papilloma(5)	88%	80%			
Papilloma(5) vs Dysplasia(7)	100%	100%			
Dysplasia(7) vs ESCC(6)	86%	100%			
ESCC(6) vsWDSCC(5)	100%	100%			

Number of samples examined is given in parenthesis

Analyst Accepted Manuscript

CAPTIONS

Fig. 1. Schematic of the experimental instrumentation for *in vivo* fluorescence measurements. The arrows represent the direction of excitation and emission light.

Fig. 2. Normalized average fluorescence emission spectra of normal and DMBA treated skin lesions under different stages of tissue transformation conditions such as (a) hyperplasia, (b) papilloma, (c) dysplasia, (d) ESCC, (e) WDSCC with their corresponding difference spectrum at 405 nm excitation.

Fig. 3. Normalized average fluorescence excitation spectra of normal and DMBA treated skin lesions under different stages of tissue transformation conditions such as (a) hyperplasia, (b) papilloma, (c) dysplasia, (d) ESCC, (e) WDSCC with their corresponding difference spectrum at 635 nm emission.

Fig. 4. H & E stained mouse skin before and after DMBA application. (a) Normal mouse skin without any DMBA application. The arrow marks shows normal epidermis and dermis with numerous hair follicles, (b) Hyperplasia. The bracket shows an increased thickness of epithelium which indicates moderate hyperplasia (c) Papilloma. It indicates papillomatous proliferation of the epidermis with hyperkeratinisation (d) Dysplasia. Dysplastic stratified squamous epithelium. The arrow shows hyperchromatic stained nucleus and dysplastic basal cells (e) Early invasive squamous cell carcinoma (ESCC). The arrow marks indicates dysplastic epithelial basal cells breaching the basement membrane forming epithelial island. (f) Well differentiated squamous cell carcinoma(WDSCC). It shows atypical mitotic figures and keratin pearls formation. The scale bar shown in the pictures corresponds to 50 μm.

Fig. 5. Scatter plot for intensity ratio of I_{580}/I_{635} at 405 nm excitation for Normal (●), Hyperplasia (□), Papilloma (▲), Dysplasia (◇), ESCC (■) and WDSCC (○) correlating with histopathologic results of the 36 mice skin. The discrimination value (1.07) separates hyperplasia from normal, the discrimination value (0.97) separates papilloma from hyperplasia, the discrimination value (0.81) separates dysplasia from papilloma, discrimination value (0.63) separates ESCC from dysplasia, and the discrimination value (0.55) separates WDSCC from ESCC.

Fig. 6. Scatter plot for intensity ratio of I_{420}/I_{515} at 635 nm emission for Normal (●) and WDSCC (■) correlating with histopathologic results of the 10 mice skin. The discrimination value (3.82) separates WDSCC from normal.

Fig. 7. Normalized average overall emission spectrum of normal and different tissue transformation of mice skin at 405 nm excitation. The arrow indicates the increasing porphyrin emission as a function of different tissue transformation.

Analyst Accepted Manuscript

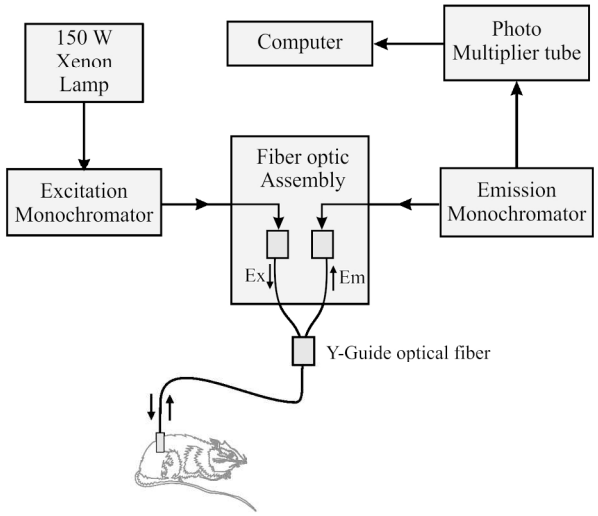

Fig. 1 Schematic of the experimental instrumentation for *in vivo* fluorescence measurements. The arrows represent the direction of excitation (Ex) and emission (Em) light.

182x143mm (300 x 300 DPI)

Analyst Accepted Manuscript

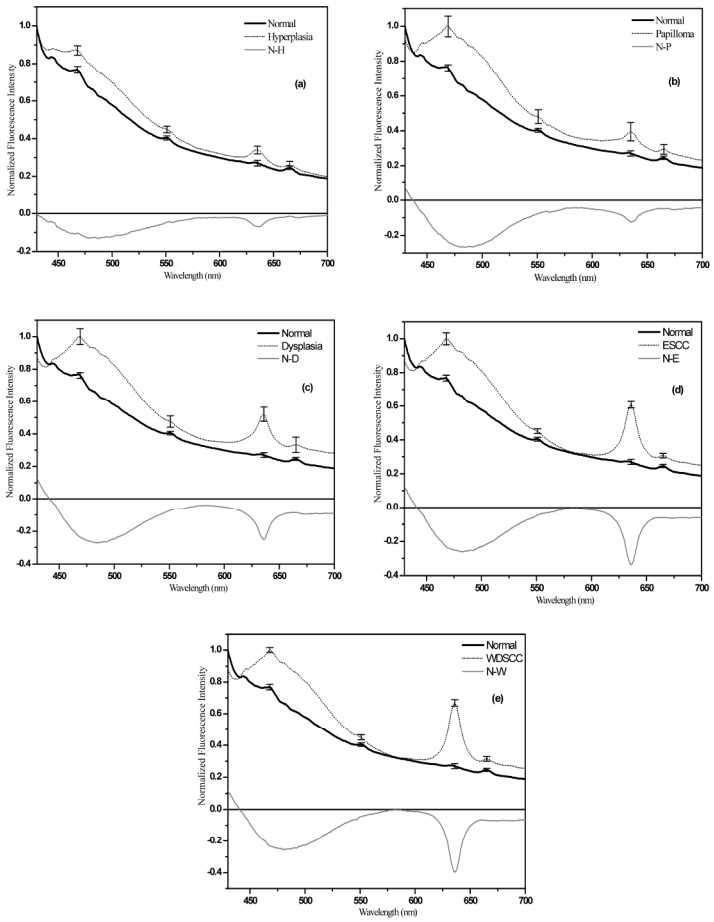

Fig. 2 Normalized average fluorescence emission spectra of normal and DMBA treated skin lesions under different stages of tissue transformation conditions such as (a) hyperplasia, (b) papilloma, (c) dysplasia, (d) ESCC, (e) WDSCC with their corresponding difference spectrum at 405 nm excitation.

196x263mm (300 x 300 DPI)

Analyst Accepted Manuscript

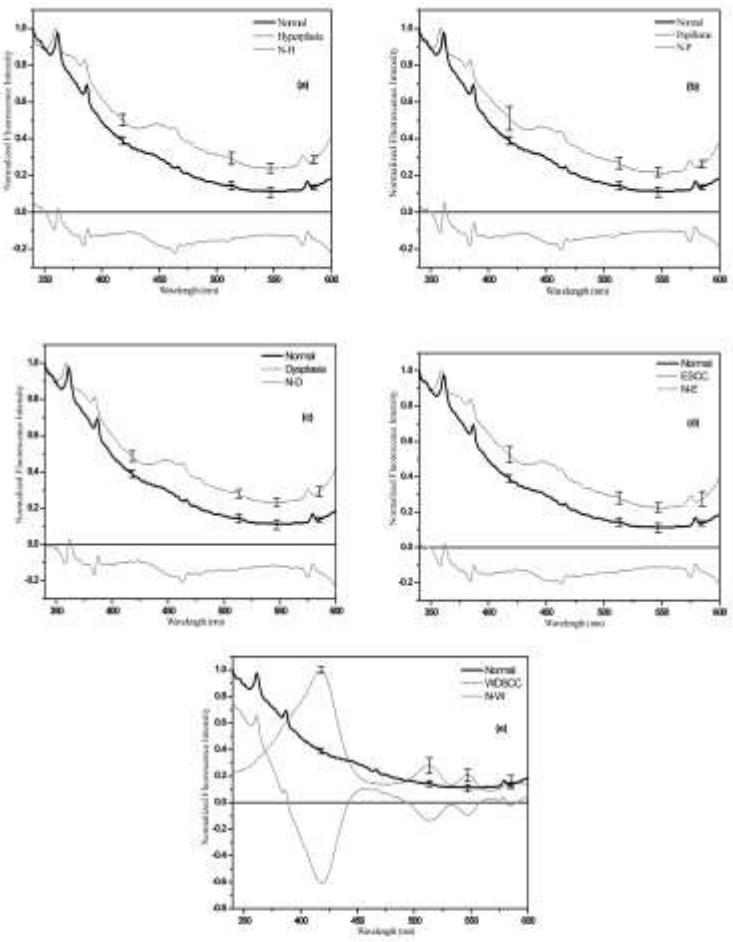

Fig. 3 Normalized average fluorescence excitation spectra of normal and DMBA treated skin lesions under different stages of tissue transformation conditions such as (a) hyperplasia, (b) papilloma, (c) dysplasia, (d) ESCC, (e) WDSCC with their corresponding difference spectrum at 635 nm emission.

184x260mm (300 x 300 DPI)

Analyst Accepted Manuscript

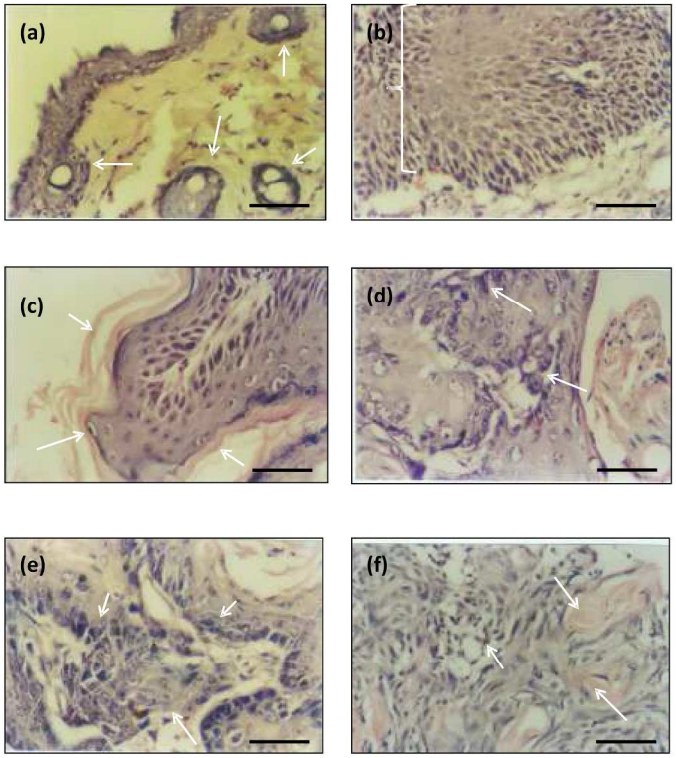

Fig. 4 H & E stained mouse skin before and after DMBA application. (a) Normal mouse skin without any DMBA application. The arrow marks shows normal epidermis and dermis with numerous hair follicles, (b) Hyperplasia. The bracket shows an increased thickness of epithelium which indicates moderate hyperplasia (c) Papilloma. It indicates papillomatous proliferation of the epidermis with hyperkeratinisation (d) Dysplasia. Dysplastic stratified squamous epithelium. The arrow shows hyperchromatic stained nucleus and dysplastic basal cells (e) Early invasive squamous cell carcinoma (ESCC). The arrow marks indicates dysplastic epithelial basal cells breaching the basement membrane forming epithelial island. (f) Well differentiated squamous cell carcinoma (WDSCC). It shows atypical mitotic figures and keratin pearls formation. The scale bar shown in the pictures corresponds to 50 μm.

188x257mm (300 x 300 DPI)

Analyst Accepted Manuscript

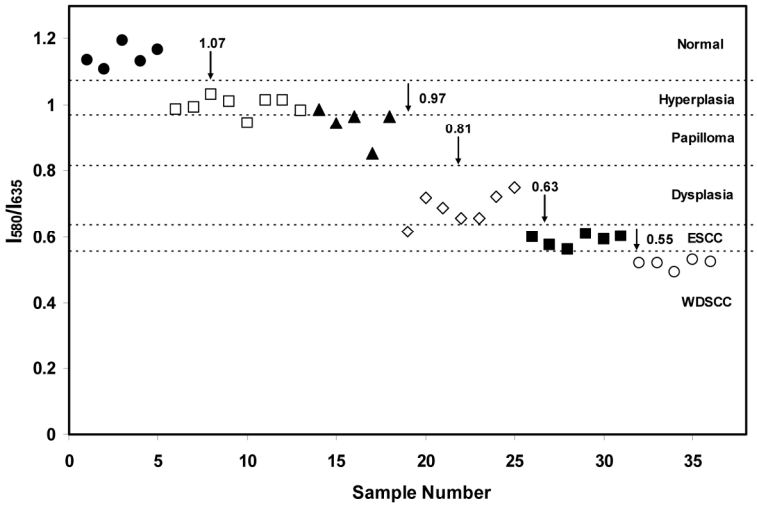

Fig. 5 Scatter plot for intensity ratio of I_{580}/I_{635} at 405 nm excitation for Normal (●), Hyperplasia (□), Papilloma (▲), Dysplasia (◇), ESCC (■) and WDSCC (○) correlating with histopathologic results of the 36 mice skin. The discrimination value (1.07) separates hyperplasia from normal, the discrimination value (0.97) separates papilloma from hyperplasia, the discrimination value (0.81) separates dysplasia from papilloma, discrimination value (0.63) separates ESCC from dysplasia, and the discrimination value (0.55) separates WDSCC from ESCC.

178x170mm (300 x 300 DPI)

Analyst Accepted Manuscript

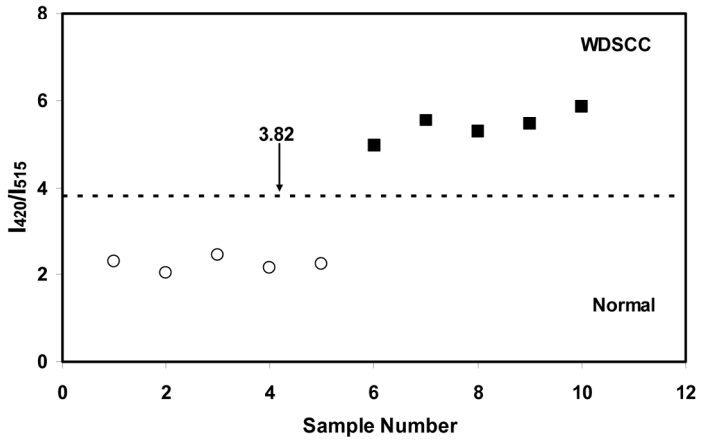

Fig. 6 Scatter plot for intensity ratio of I_{420}/I_{515} at 635 nm emission for Normal (●) and WDSCC (■) correlating with histopathologic results of the 10 mice skin. The discrimination value (3.82) separates WDSCC from normal.

174x137mm (300 x 300 DPI)

Analyst Accepted Manuscript

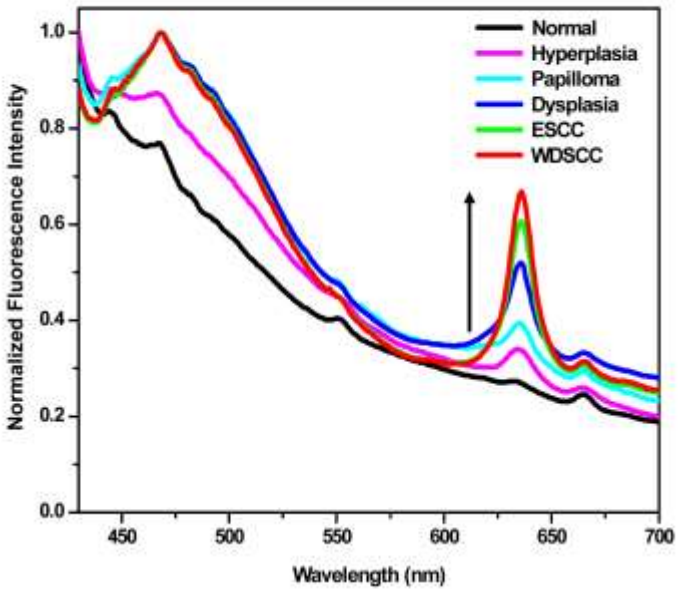

Fig. 7 Normalized average overall emission spectrum of normal and different tissue transformation of mice skin at 405 nm excitation. The arrow indicates the increasing porphyrin emission as a function of different tissue transformation.

170x166mm (300 x 300 DPI)

Analyst Accepted Manuscript